*Chemistry, Physics and Technology of Surface. 2024. V. 15. N 4. P. 456-466*

*UDC 539* doi: 10.15407/hftp15.04.456

**Faris M.A. Al-Hamdany [1], Abdulkhaliq A. Sulaiman [2], Abdullah I.M. Alabdullah [3]**

# STUDY OF THE PERFORMANCE OF ORGANIC SOLAR CELLS USING $SnO_2$ NANOPARTICLES AS ELECTRON TRANSPORT LAYER GROWTH BY PULSED LASER DEPOSITION

*[1] Ninevah University, Mosul, Iraq, E-mail: faris.ahmed@uoninevah.edu.iq*
*[1,2, 3] Department of Physics, College of Science, Mosul University, Mosul, Iraq*
*E-mail: dr.abdulkhalaq@uomosul.edu.iq, abdullahidrees@uomosul.edu.iq*

*The electron transport layer (ETL) material plays a crucial role in determining the device efficiency and stability of organic solar cells (OSCs). Tin oxide ($SnO_2$) semiconductor is commonly used as ETL in organic solar cells and recently has attracted significant attention. In this paper $SnO_2$ particles deposited by pulsed laser deposition (PLD) are used as ETL layer in inverted organic solar cells with structure (FTO/$SnO_2$/PTB7-Th:O-IDTBR/ $MoO_3$/Ag). The characterizations of cell using the Ossila Solar Cell I-V Test System have been investigated as well as the structural properties of $SnO_2$ thin film using a Field emission scanning electron microscope (FESEM), The atomic force microscopy (AFM) and X-ray spectrum have been also investigated. It has been found that the Power conversion efficiency (PCE) of solar cell is 15.08 %. The stability was measured for 30 min with continuous illumination under the ambient air conditions, it was decreasing gradually over the illumination period to about half initial value of efficiency. The FESEM images and XRD spectrum show that the films were crystalline. The XRD spectrum shows the presence of several peaks belonging to $SnO_2$ nanoparticles. The optical properties of $SnO_2$ film indicate the increase in the transmittance and refractive index spectrum, while the absorbance spectrum decreases, the maximum absorbance was observed at 320 nm wavelength and the optical energy gap record about 3.1 eV and the grain size for $SnO_2$ reported around 20–60 nm.*

***Keywords**: organic solar cell, $SnO_2$, electron transport layer, pulsed laser deposition, solar cell characterization, stability*

## INTRODUCTION

OSCs classified as third-generation photovoltaic thin-film, they have potential cost-effectiveness and lightweight characteristics and developing photovoltaic technology [1].

First single-layer organic photovoltaic cell was introduced by Kearns and Calvin in 1958 [2]. The maximum output power was only $3\times10^{-12}$W as a result of the insufficient charge separation, notwithstanding a PCE that remained below 0.1 %. The challenge was in attaining effective segregation of exciton (electron-hole pairs) and facing a substantial rate of electrons and holes recombination [3]. Tang in 1986 introduced the first bilayer solar cell, which had a low PCE of just 1 % due to inadequate charge transfer and a limited interfacial area [4].

Organic solar cells consist of multiple layers built on a conducting semi-transparent substrate layer such as FTO or ITO-coated glass which acts as an electrode and allows light to pass through. The photoactive layer is responsible for harvesting light and consists of a polymer that acts as a donor and small molecules that act as acceptors which are organic semiconductor materials, this layer is located between the hole transport layer (HTL) and electron transport layer (ETL) which are the interfacial layers. On the top is a metal electrode for charge collection which could be either an anode or cathode depending on whether the device structure is conventional or inverted [5]. Enhancing the overall performance of OSCs is contingent upon optimizing both efficiency and a long lifespan [6]. To overcome these limitations, the researchers are trying to using diverse techniques to enhance efficiency and lifespan. These techniques include deposition techniques, altering the martial implementing low-cost fabrication methods, concentrations of the photoactive layer, classification, altering the material of the photoactive layer, designing inverted structures instead of conventional ones, encapsulation, substituting photoactive materials, changing of ETL materials, adjusting the blend ratio of donor and acceptor, utilizing bulk

heterojunction solar cells (BHJ–OSCs) configuration for the active layer, encapsulation [7–8]. Based on the composition of the active layer, OSCs can be classified into a tandem structure, ternary, bulk heterojunction (BHJ), bilayer, and single layer [9].

Heeger and his colleagues established the concept of bulk heterojunction (BHJ) in 1995 to address issues such as poor lifetime and limited exciton diffusion length [10]. The BHJ includes a blend of donor and acceptor materials. Creating an interconnected network with an extensive interfacial area promotes effective exciton dissociation. This increase in exciton separation distance has notably enhanced device performance. Currently, bulk heterojunction organic solar cells (BHJ–OSCs) are attaining PCEs approaching up to 20 %, this marks a revolutionary advancement in the field of OSCs and solidifies their standing as a promising photovoltaic technology [11, 12]. After more than ten years of research development it still exhibits relatively low power conversion efficiency (PCE) of around 23 % [13].

The ETL plays an important role in improving the performance of OSCs [14]. Metal oxides with low work functions are usually used as the ETL in OSCs with an inverted structure [15], $SnO_2$ is a commonly employed as electron transport layer materials due to their stability, ease of production and capacity to change their energy band structure. The main roles of these materials are to (1) aid in the transfer of electrons to the electrode layer, (2) hinder the movement of holes toward the cathode electrode and (3) act as a barrier to prevent unwanted interactions between layers while controlling the energy levels between the electrode and the photoactive layer [16]. Recently $SnO_2$ has attracted considerable interest as an ETL in OSCs because of its superior electron mobility, high charge extraction, resistance to ultraviolet radiation, superior band alignment, reduced photocatalytic activity and exceptional chemical stability in comparison to other with other metal oxides such as ZnO and $TiO_2$ [4, 17]. There are three primary main type of nanostructures in solar cells: firstly, zero-dimensional structures are primarily nanoparticles and quantum dots, secondly one-dimensional structures are primarily nanoribbons, nanotubes, nanorods and nanowires and thirdly two-dimensional structures are primarily ultra-thin films multilayer thin films [18]. Various nanostructures of metal oxide materials are commonly utilized in electron transport layers, such as nanoparticle structures, nano-rod structures, branching nano-rod structures, and porous single-crystal structures [16].

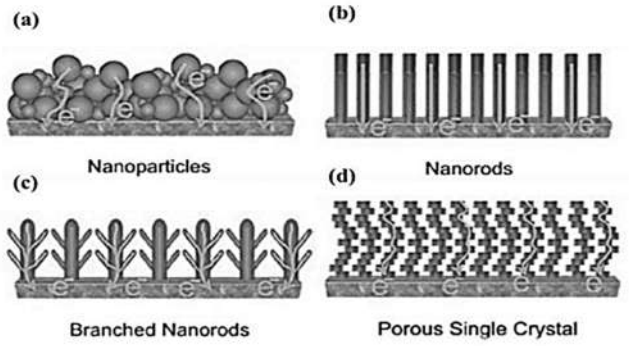


**Fig. 1.** The most common structures of nanostructured metal oxide using as an ETL in OSCs, (*a*) nanoparticles, (*b*) nanorods, (*c*) branching nanorods and (*d*) porous single-crystal [16]

$SnO_2$ nanoparticles recently are extensively utilized as electron transport layer for organic solar cells. $SnO_2$ is well recognized for its high transparency, superior electrical properties, conductivity, and suitability for low-temperature processing, excellent chemical stability, making it an appropriate material for organic solar cell fabrication [4, 16, 19].

The deposition of $SnO_2$ thin film layer as ETL can be done through the utilization of various techniques from chemical depositions such as sol-gel process, chemical bath deposition (CBD) [20], chemical vapor deposition (CVD) and metal-organic chemical vapor deposition (MOCVD) to physical depositions, such as pulsed laser deposition (PLD), thermal evaporation,

magnetron sputtering, sputtering, spray deposition [21], spin-coating, radio frequency sputtering, physical vapor deposition, ink-jet printing, electrodeposition and atomic layer deposition [22–24].

In the OSCs fabrication, $SnO_2$ are often obtained through solution processing which offers advantages in terms of cost-effectiveness and scalability, as it uses colloidal dispersions of nanoparticles to deposit through solution processing. It is limited in its ability to alter the properties of the ETL, particularly those related to conductivity and crystallinity. In addition, the defects may be created as a result of the remaining of residual organic ligands and additives which stabilize the colloidal dispersion [15, 25, 26]. As a result, this generates an interface that has a poor adhesion with the active layer, which in turn lead to an increasing the possibility of losses in energy and hence reducing overall performance [27]. PLD which has been several benefits associated with its utilization to produce ETL, these benefits include compatibility with large-scale production, patentability, and the capacity to achieve rapid deposition rates [21, 28].

In this study, inverted organic solar cell has been fabricated with BHJ active layer using $SnO_2$ nanoparticles as ETL, which was deposited by pulsed laser deposition. The efficiency and degradation time of the cell was measured. The optical properties, morphology and surface topography of $SnO_2$ materials have been also investigated.

## MATERIALS AND METHODS

***Materials.*** The glass fluorine-doped tin oxide slides (FTO) with (2 cm×2 cm×1.1 mm) size and sheet resistance (9 Ω/sq) were purchased from Chemical Point, Germany. Tin Oxide $SnO_2$ and Molybdenum trioxide ($MoO_3$) nanoparticles were purchased from US Research Nanomaterials, Inc. The donor polymer (PTB7-Th) and *n*-type non-fullerene electron acceptor (O-IDTBR) were purchased from Ossila Co., UK. The solvent chlorobenzene from the College of Science Lab, University of Mosul. Finally, Silver (Ag) is commercial with a purity percentage (99.1 %). The chemical structures of the polymer (PTB7-Th) (donor) and non-fullerene (acceptor) (O-IDTBR) are shown in Fig. 2.

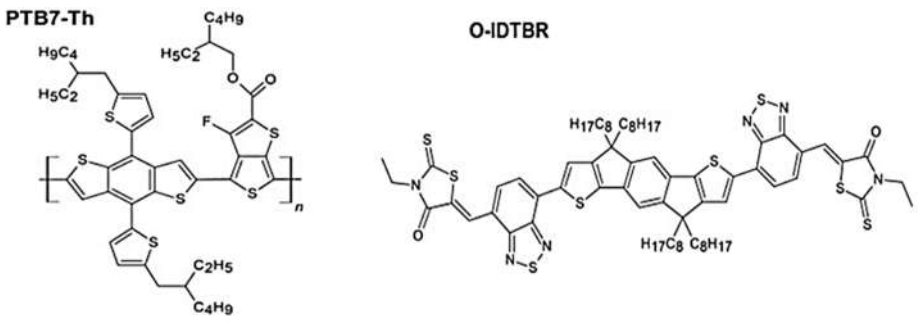


**Fig. 2.** The schematic representation of chemical structures of the studied polymer (PTB7-Th) (donor) and non-fullerene (acceptor) (O-IDTBR) [27]

***Device Structures.*** The structure of the inverted organic solar cell based with bulk heterojunction active layer (BHJ) configuration consists of many layer materials including glass FTO as a cathode, $SnO_2$ NPs as ETL, the photoactive layer (active layer) blend of PTB7-Th polymer as a donor and O-IDTBR non-fullerene as an acceptor, $MoO_3$ as HTL and Ag as an anode. As shown in Fig. 3, our examined semitransparent inverted bulk-heterojunction-type PTB7-Th: O-IDTBR organic solar cells were arranged in a stack from the bottom to the top.

***Device Fabrication.*** As shown in Fig. 4 the two inverted structure organic solar cells were fabricated with a (1:1) blend ratio of donor and accepter (PTB7-Th:O-IDTBR) photoactive layer as a BHJ fabricated one structure of (glass FTO/ $SnO_2$ ETL/PTB7-Th:O-IDTBR /$MoO_3$/Ag). At the beginning, the FTO-coated glass conducting slide substrate with (2 cm×2 cm×1.1 mm) size with sheet resistance (15 Ω/sq) and cleaned by ultrasonically with de-ionized water, acetone, ethanol, and isopropanol for 15 min each and finally left to dry by air gun. Then 0.9 g of $SnO_2$

NPs powder as an ETL was deposed on FTO-coated glass substrate by PLD technique. Further, the PTB7-Th nanoparticle powder dissolved in chlorobenzene and stirred for 2 h with a solution concentration of 25 mg/ml and the same process was performed for O-IDTBR, both solutions then mixed with a blend ratio (1:1) to make the BHJ active layer solution**.** The blend ratio solution was stirred for 1 h and deposited by spin coating on the (FTO/ETL $SnO_2$) substrate with a two-step rate speed (350 rpm for 10 s and 2000 rpm for 30 s) in the ambient atmosphere to make 100 nm. $MoO_3$ HTL for 50 nm and 100 nm for Ag electrode were deposited by the thermal evaporation technique under a vacuum chamber $7.9\times10^{-5}$ and $6.4\times10^{-5}$ mbar respectively.

The $SnO_2$ powder partials deposited by (PLD) using (Nd:YAG Laser) with constant power (1000 mJ) and laser frequency set at 6 Hz. The Chamber pressures on the order of ($10^{-4}$ mbar) as shown in Fig. 5.

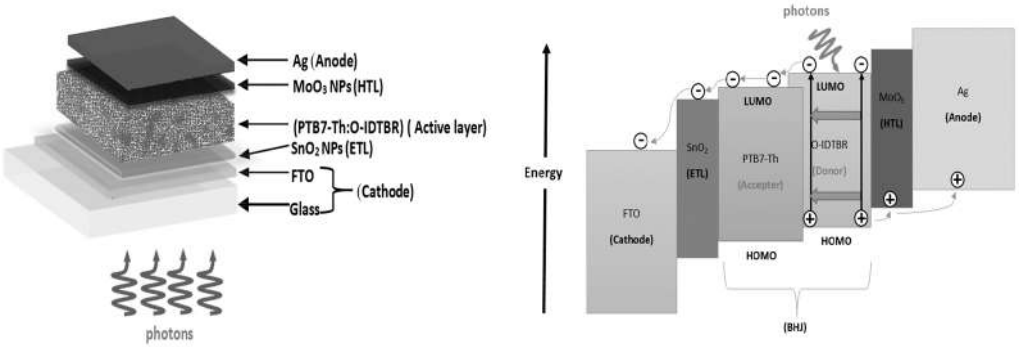


*a* *b*

**Fig. 3.** Schematic representation the inverted organic solar cell: *a* – the device structure (Glass FTO/ $SnO_2$ /PTB7-Th: O-IDTBR/ $MoO_3$/Ag), *b* – the diagram of electronic processes that occur under the influence of light


*a* *b*

**Fig. 4.** Schematic representation of (*a*) pulsed laser deposition setup, (*b*) the laser energy power (1000 mJ) with frequency at 6 Hz

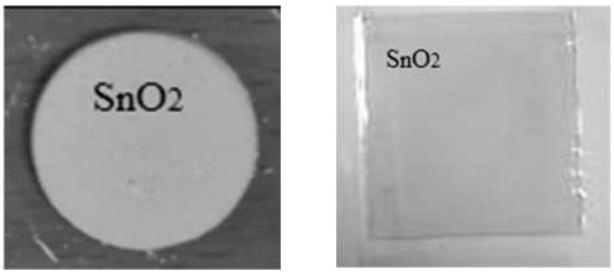


*a* *b*

**Fig. 5.** *a* – the desk of $SnO_2$ powder after pressed under 6 tons for 15 min which is represent the target deposition, *b* – the $SnO_2$ deposited by PLD on the FTO glass

## RESULTS AND DISCUSSION

***Optical properties of $SnO_2$ thin film.*** The optical properties of $SnO_2$ thin film deposited on glass by pulsed laser deposition have been investigated. Fig. 6 illustrates the optical characteristics of $SnO_2$ thin films. With incident wave at room temperature over the visible wavelength, the transmittance and refractive index spectrum increases, in contrast the absorbance spectrum decreases. The maximum absorbance of $SnO_2$ thin film has been observed at 320 nm wavelength. The optical energy gap value of $SnO_2$ thin film was about 3.1 eV and there is a blue shift of energy gap and this occurred may be for two reasons. Firstly, we used 200 laser repetitions and the energy gap decrease with higher pulse laser repetitions and this is in agreement with data in [29]. Secondly, the energy gap decreases with higher laser energy and we used (1000 mJ) and this is in agreement with data in [30].

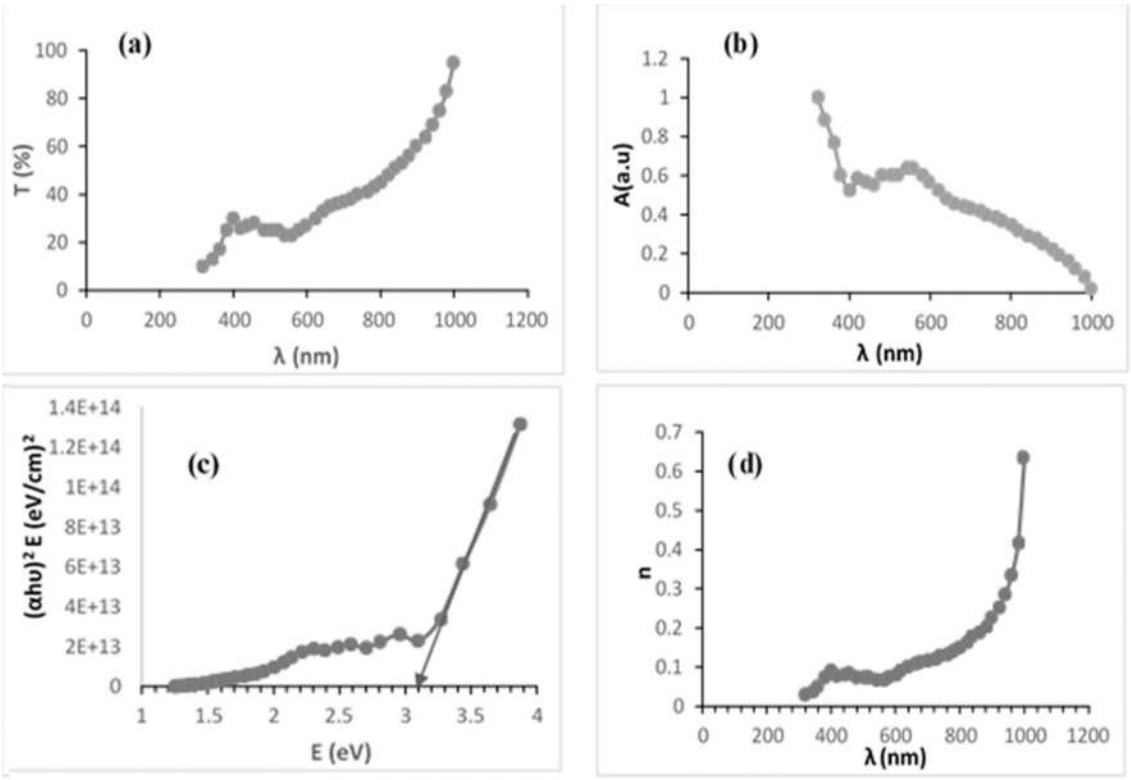


**Fig. 6.** The optical properties and the energy gap of $SnO_2$ thin film (*a*), transmission (*b*), absorbance (*c*), energy gap (*d*) refractive index

***X-ray Diffraction Analysis (XRD).*** The XRD patterns of $SnO_2$ film (Fig. 7) shows a narrow and distinctive sharp peaks with high intensity singles at diffraction angles (2θ °) 26.42 °, 33.70 °, 51.61° corresponding to orientation (110), (101) and (211). There are another low intensity peaks appeared at diffraction angles (2θ °) 37.77 °, 38.81 °, 42.44 °, 54.59 °, 57.67 °, 61.72 °, 64.57 °, 65.80 °, 71.12 ° and 78.56 ° corresponding to orientation (200), (111), (210), (220), (002), (310), (112), (301), (202), (321) respectively and show body cubic center structure. These results are showing complete agreement with the data of the Joint Committee on Powder Diffraction Standards (JCPDS No. 01-0657) [31].

The shape morphology and surface topography of material particles examined in this study are evaluated using Field Emission Scanning Electron Microscopy (FESEM) and Atomic Force Microscopy (AFM).

The images of FESEM for the surface of (PTB7-Th) donor polymer, (O-IDTBR) non-fullerene acceptor films and the mixed of them with a blend ratio of 1:1 film are illustrated in Fig. 8. The images indicate the size of the grains were within the nanoscale for both active layer materials.

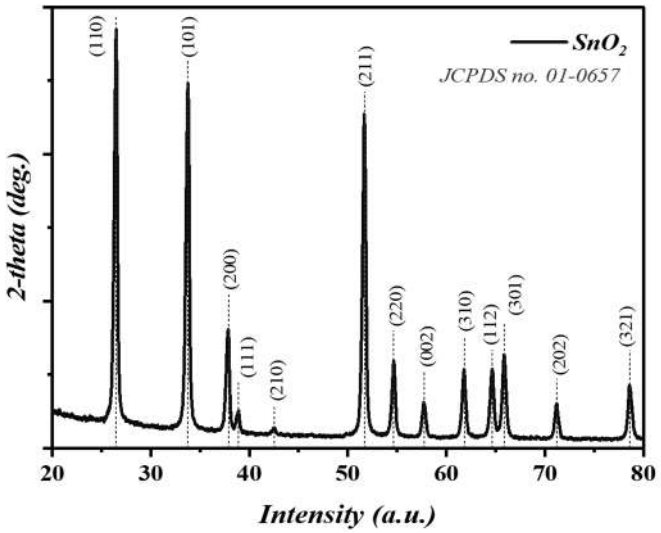


**Fig. 7.** XRD patterns of phase-pure $SnO_2$ nanoparticles film

**Table 1.** The diffraction angles (2θ), full-width at half-maximum (FWHM) of profile peaks and the average grain size of $SnO_2$ deposited on FTO-coated glass

| Average grain size, nm | Pos. [2θ] | FWHM Left [2θ] | D, nm |
|---|---|---|---|
| | 26.4284 | 0.1609 | 50.72151633 |
| | 33.7017 | 0.3828 | 21.68573785 |
| | 37.7787 | 0.3726 | 22.53618791 |
| | 38.8148 | 0.3754 | 22.43835863 |
| | 42.4458 | 0.4061 | 20.98659745 |
| | 51.6123 | 0.1803 | 48.94278252 |
| 28.449938 | 54.593 | 0.3436 | 26.01778945 |
| | 57.6741 | 0.3757 | 24.13805565 |
| | 61.7285 | 0.3517 | 26.31362351 |
| | 64.5718 | 0.3521 | 26.68719288 |
| | 65.8097 | 0.38 | 24.89899295 |
| | 71.1246 | 0.3713 | 26.29872304 |
| | 78.5634 | 0.3641 | 28.18364726 |


*a* *b* *c*

**Fig. 8.** Field emission scanning electron microscopy (FESEM) of (*a*) PTB7-Th donor polymer, (*b*) O-IDTBR non-fullerene acceptor films and (*c*) mixed film of donor and acceptor with a blend ratio of 1:1

The grains size of $SnO_2$ powder deposited on FTO glass varied from 20–380 nm as a result of the grow and aggregation of the grains, average size of them was between 20–80 nm as showing in the Fig. 9, and this agree with FESEM image and XRD spectrum.

The Atomic force microscopy (AFM) revealed the root-mean-square (RMS) of around 3.408 nm for over (6.87×6.87) μm$^2$ for $SnO_2$ as indicated in Table 2 and Fig. 10.

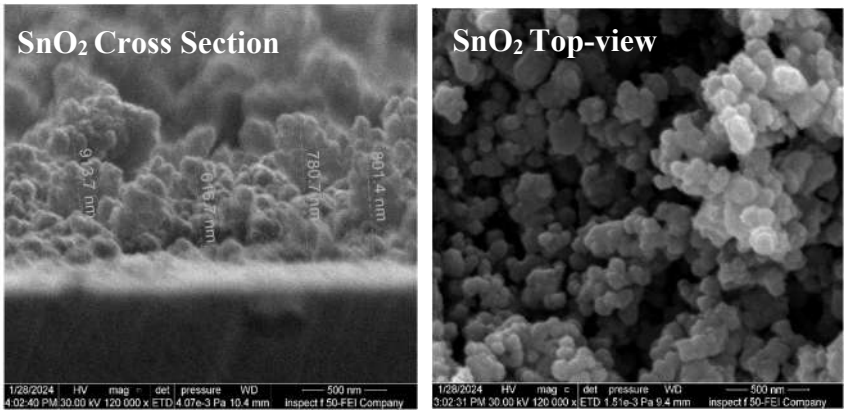


**Fig. 9.** The high-resolution images of Cross-sectional SFEEM images and Top-view at (w120 kx magnification) for $SnO_2$ NPs film deposited on FTO glass substrate by PLD

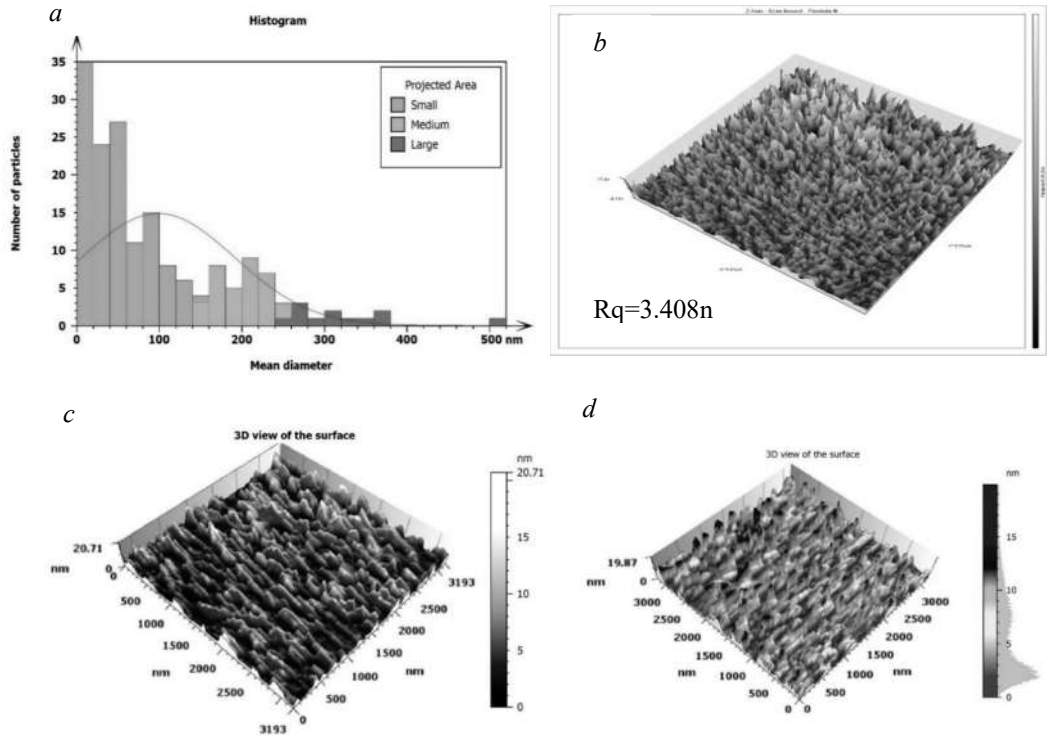


**Fig. 10.** The (AFM) images of $SnO_2$ film (*a*) the (RMS) over the (6.87×6.87) μm$^2$ area (*b*) the number of the particles as a function of diameter indicate the particle diameter of ZnO varied from 20–80 nm and this agreement with (FESEM) images and (XRD) analysis (*c*) and (*d*) the 3D view of $SnO_2$ film surface

**Table 2.** The Root-mean-square height 3.408 nm, maximum height 19.87 nm and the arithmetic mean height 2.923 nm

| Height parameters | | | |
|---|---|---|---|
| Sq | 3.408 | nm | Root-mean-square height |
| Ssk | 0.7848 | | Skewness |
| Sku | 2.705 | | Kurtosis |
| Sp | 14.78 | nm | Maximum peak height |
| Sv | 5.093 | nm | Maximum pit depth |
| Sz | 19.87 | nm | Maximum height |
| Sa | 2.923 | nm | Arithmetic mean height |

***Electrical Properties.*** The current density-voltage (J-V) characteristic curves as well as the degradation time of the fabricated cell were assessed using the Ossila Solar Cell I-V Test System. This system incorporates the solar simulator in a combination source measure unit as well as a test board, I-V Solar Cell Software, and illuminates the devices with light having an AM 1.5 G and grade A spectral distribution of the light intensity, calibrated to 1000 W/m$^2$, was verified using a certified reference solar cell.

Tin oxide nanoparticles as ETL have been used in the preparation of eight solar cells to ensure quantitative measurements of J-V characteristic under the standard illumination conditions (AM 1.5 G, 1000 W/m$^2$). The cells parameters are shown in Table 3 and Fig. 11.

**Table 3.** Parameters performance of OSCs with $SnO_2$ NPs ETL

| Organic Solar Cell Structure | ETL Type | $J_{SC}$ (mA/ cm$^2$) | $V_{OC}$ (V) | FF | PCE (%) |
|---|---|---|---|---|---|
| FTO/ $SnO_2$ /PTB7-Th:O-IDTBR)/ $MoO_3$/Ag | $SnO_2$ | 25.164 | 0.889 | 0.67 | 15.08 |

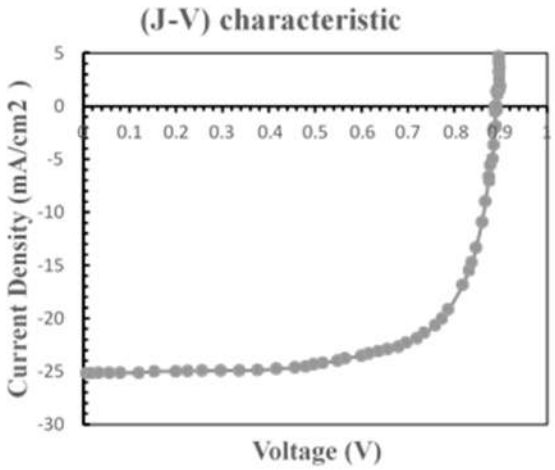


**Fig. 11.** The J-V characteristic curves of inverted organic solar cell for (FTO/$SnO_2$/PTB7-Th: O-IDTBR)/$MoO_3$/Ag)

The high PCE of OSCs using $SnO_2$ NPs as ETL can be ascribed due to $SnO_2$ has a higher conductivity [8], strong charge extraction [13], wider bandgap (3.4–4.3) eV, excellent electrical and optical properties, high transmittance in the UV–visible region and [29] and finally $SnO_2$ possess a higher electron mobility up to 400 cm$^2$ V s$^{-1}$ [32].

***Solar Cell Stability.*** The organic solar cells with structure (FTO/$SnO_2$ NPs/PTB7-Th:O-IDTBR)/ $MoO_3$/Ag) under continuous illumination (AM. 5G, 1000 W/m$^2$) in ambient conditions shows that the efficiencies decreased with illumination time from 15.08 % to 11.5 % as listed in Table 4.

Fig. 12 indicates the performance of OSCs with $SnO_2$ ETL, it shows a slow degradation in

the efficiency after continuous light illumination for 30 min, this decrease in efficiency may be result from the low photocatalytic activity of $SnO_2$ which has sufficient energy levels for the effective extraction of electrons from the majority of non-fullerene acceptors, wide band gap of 3.50 eV, excellent chemical stability, superior transparency to visible light, higher electron mobility and high resistance against UV radiation due to its wider band gap which produce a decomposition of the active layer materials, for this reason $SnO_2$ has been widely used to reach high performance in OSCs [4, 13, 29, 32].

**Table 4.** The efficiencies as a function of continuous illumination time of organic solar cells using $SnO_2$ ETL during the experiment under continuous illumination (AM 1.5G,1000 W/m$^2$) under ambient conditions

| Time (min) | Organic Solar cell PCE (%) with $SnO_2$ as ETL |
|---|---|
| 0.031 | 15.08689 |
| 5 | 13.35729 |
| 10 | 11.99451 |
| 15 | 10.96761 |
| 20 | 9.88791 |
| 25 | 8.9813 |
| 30 | 8.5584 |

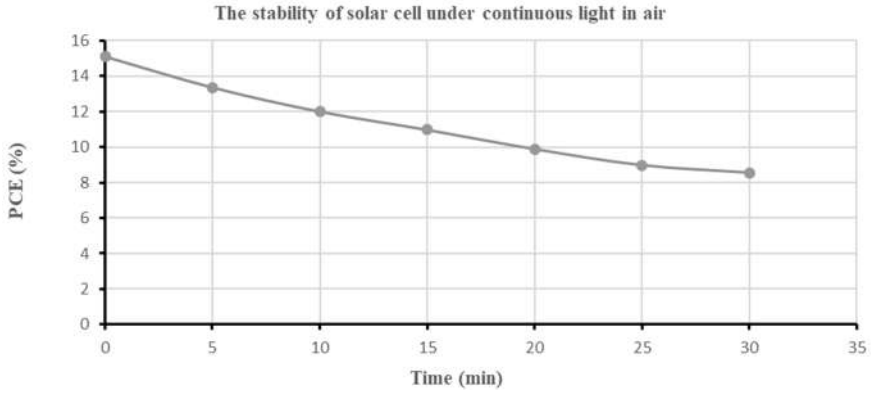


**Fig. 12.** The PCE value for OSCs using $SnO_2$ NPs as a function of soaking time light illumination including UV radiation (AM 1.5G illumination,1000 W/m$^2$) for 35 minutes

## CONCLUSION

The electron transport layer metal oxide and its impact on the efficiency and lifetime of organic solar cell has been investigated. The organic solar cells with inverted structure based on bulk heterojunction active layer have been constructed with structure (FTO/$SnO_2$/PTB7-Th:O-IDTBR/$MoO_3$/Ag) using $SnO_2$ nano-particles as electron transport layer deposited using pulsed laser deposition. The optical properties of $SnO_2$ film show the increases of transmittance and refractive index spectrum, while the absorbance spectrum decreases, the maximum absorbance at 320 nm and the optical energy gap record about 3.1 eV. The X-ray spectrum of $SnO_2$ film shows a narrow and distinctive sharp peaks with high intensity singles and other low intensity singles peaks. The current density – voltage characteristic diagram of organic solar cells show that the maximum power conversion efficiency recorded is (15.08 %). The stability of organic solar cells under continuous illumination in air indicated that the cell exhibit higher operational stability when exposed to light while the efficiency decreases from (15.08 %) to (8.55 %). The results of our research demonstrated that $SnO_2$ nanoparticles are considered to be an acceptable alternative to other metal oxide using as electron transport layer for an organic solar cell's bulk heterojunction active layer and a non-fullerene acceptor.

# Дослідження роботи органічних сонячних елементів з використанням наночастинок $SnO_2$ для наростання електронного транспортного шару шляхом імпульсного лазерного осадження

**Faris M.A. Al-Hamdany, Abdulkhaliq A. Sulaiman, Abdullah I.M. Alabdullah**

*Університет Ніневі, Мосул, Ірак, faris.ahmed@uoninevah.edu.iq*
*Факультет фізики, науковий коледж, Мосульський університет, Мосул, Ірак*
*dr.abdulkhalaq@uomosul.edu.iq, abdullahidrees@uomosul.edu.iq*

*Матеріал шару транспортування електронів (ETL) відіграє вирішальну роль у визначенні ефективності та стабільності пристроїв органічних сонячних елементів (OSC). Напівпровідник на основі оксиду олова ($SnO_2$) зазвичай використовується як ETL в органічних сонячних елементах (OSC) і останнім часом привернув значну увагу. У цій статті частинки $SnO_2$, осаджені за допомогою імпульсного лазерного осадження (PLD), використовуються як шар ETL в інвертованих органічних сонячних елементах зі структурою (FTO/$SnO_2$/PTB7-Th:O-IDTBR/$MoO_3$/Ag). Досліджені характеристики елемента за допомогою тестової системи Ossila Solar Cell I-V, а також структурні властивості тонкої плівки $SnO_2$ за допомогою скануючого електронного мікроскопа (FESEM), атомно-силової мікроскопії (AFM) і рентгенівської спектроскопії. Було встановлено, що ефективність перетворення енергії (PCE) сонячної батареї становить 15.08 %. Стабільність вимірювали протягом 30 хвилин при безперервному освітленні на повітрі, вона поступово знижувалася протягом періоду освітлення приблизно до половини початкового значення ефективності. Зображення FESEM і XRD-спектр показують, що плівки були кристалічними. XRD-спектр показує наявність кількох піків, що належать наночастинкам $SnO_2$. Оптичні властивості плівки $SnO_2$ вказують на збільшення спектра коефіцієнта пропускання та показника заломлення, у той час як спектр поглинання зменшується, максимальне поглинання спостерігалося при довжині хвилі 320 нм, оптичний енергетичний проміжок становив близько 3.1 еВ, а розмір зерен для $SnO_2$, становить приблизно 20–60 нм.*

***Ключові слова**: Органічний сонячний елемент, $SnO_2$, транспортний шар електронів, імпульсне лазерне осадження, характеристики сонячних елементів, стабільність*

REFERENCES

1. Soonmin H., Hardani Nandi P., Mwankemwa B.S., Malevu T.D., Malik M.I. Overview on different types of solar cells: an update. *Appl. Sci*. 2023. **13**(4): 2051.
2. Husen M.J., Aga F.G., Dibaba S.T. Theoretical Performance Analysis of Inverted P3HT: PCBM Based Bulk Hetero-Junction Organic Solar Cells through Simulation. *Adv. Mater. Sci. Eng*. 2023. **2023**: 1.
3. Movla H., Shahalizad A., Asgari A. A numerical study on the relationship between the doping and performance in P3HT: PCBM organic bulk heterojunction solar cells. *Sci. Rep*. 2023. **13**(1): 2031.
4. Kong T., Yang G., Fan P., Yu J. Solution-Processable NiOx: PMMA Hole Transport Layer for Efficient and Stable Inverted Organic Solar Cells. *Polymers*. 2023. **15**(8): 1875.
5. Alkarsifi R., Ackermann J., Margeat O. Hole transport layers in organic solar cells: A review. *J. Met. Mater. Miner.* 2022. **32**(4): 1.
6. Tarique W.B., Uddin A. A review of progress and challenges in the research developments on organic solar cells. *Mater. Sci. Semicond. Process*. 2023. **163**: 107541.
7. Raeyani D., Asgari A. Enhancing the Efficiency of Inverted Organic Solar Cells with Treatment Techniques: Numerical and Experimental Study. *Int. J. Energy Res*. 2023. **2023**: 1.
8. Suo Z., Xiao Z., Li S., Liu J., Xin Y., Meng L., Chen Y. Efficient and stable inverted structure organic solar cells utilizing surface-modified SnO2 as the electron transport layer. *Nano Energy*. 2023. **118**: 109032.
9. Solak E.K., Irmak E. Advances in organic photovoltaic cells: a comprehensive review of materials, technologies, and performance. *RSC Adv*. 2023. **13**(18): 12244.
10. Lim F.J., Ananthanarayanan K., Luther J., Ho G.W. Influence of a novel fluorosurfactant modified PEDOT: PSS hole transport layer on the performance of inverted organic solar cells. *J. Mater. Chem*. 2012. **22**(48): 25057.
11. Mohamed El Amine B., Zhou Y., Li H., Wang Q., Xi J., Zhao C. Latest Updates of Single-Junction Organic Solar Cells up to 20 % Efficiency. *Energies*. 2023. **16**(9): 3895.

12. Tarique W.B., Uddin A. A review of progress and challenges in the research developments on organic solar cells. *Mater. Sci. Semicond. Process*. 2023. **163**: 107541.
13. Hoang Huy V.P., Bark C.W. Review on Surface Modification of $SnO_2$ Electron Transport Layer for High-Efficiency Perovskite Solar Cells. *Appl. Sci*. 2023. **13**(19): 10715.
14. Zeng L., Wang L., Qin J., Ren Y., Li H., Lu X., Li J. Applying l-cystine as an electron transport layer toward efficient organic solar cells. *Opt. Mater*. 2023. **136**: 113404.
15. Di Mario L., Romero D.G., Wang H., Tekelenburg E.K., Meems S., Zaharia T., Loi M.A. Outstanding Fill Factor in Inverted Organic Solar Cells with $SnO_2$ by Atomic Layer Deposition. *Adv. Mater*. 2024. **36**(20): 2301404.
16. Wang Y., Tan S.T. Composition of Electron Transport Layers in Organic Solar Cells (OSCs). *Highlights in Science, Engineering and Technology*. 2022. **12**: 99.
17. Kim J., Kim K.S., Myung C.W. Efficient electron extraction of $SnO_2$ electron transport layer for lead halide perovskite solar cell. *npj Comput. Mater*. 2020. **6**(1): 100.
18. Gonzalez-Valls I., Lira-Cantu M. Vertically-aligned nanostructures of ZnO for excitonic solar cells: a review. *Energy Environ. Sci*. 2009. **2**(1): 19.
19. Kong T., Wang R., Zheng D., Yu J. Modification of the $SnO_2$ electron transporting layer by using perylene diimide derivative for efficient organic solar cells. *Front. Chem*. 2021. **9**: 703561.
20. Tangade H.S., Pusawale S.N., Shirguppikar S.S. Synthesis and characterization of ZnO thin films deposited by chemical route. *Materials Today: Proceedings*. 2020. **33**(8): 5147.
21. Thomas B., Skariah B. Spray deposited Mg-doped $SnO_2$ thin film LPG sensor: XPS and EDX analysis in relation to deposition temperature and doping. *J. Alloys Compd*. 2015. **625**: 231.
22. Hong C., Kim M., Lee J.G., Shao Q., Lee H.S., Park H.H. Research of Si-ZnO Thin-Film Transistors Deposited by Atomic Layer Deposition. *Int. J. Energy Res*. 2023. **2023**.
23. Derbali L., Bouhjar F., Derbali A., Soucase B.M. Enhanced ZnO-based ETL and nanostructured interface modification for improved perovskite solar cells efficiency. *Opt. Mater*. 2023. **145**: 114440.
24. Huang S., Li P., Wang J., Huang J.C.C., Xue Q., Fu N. Modification of $SnO_2$ electron transport Layer: Brilliant strategies to make perovskite solar cells stronger. *Chem. Eng. J*. 2022. **439**: 135687.
25. Yu R., Wei X., Wu G., Zhang T., Gong Y., Zhao B., Tan Z. A. Efficient interface modification via multi-site coordination for improved efficiency and stability in organic solar cells. *Energy Environ. Sci.* 2022. **15**(2): 822.
26. Wu J., Tang F., Wu S., Li Y., Xiao L., Zhu X., Peng X. Interface Modification of Tin Oxide Electron-Transport Layer for the Efficiency and Stability Enhancement of Organic Solar Cells. *Adv. Energy Mater.* 2024. **14**(2): 2302932.
27. Clarke A.J., Luke J., Meitzner R., Wu J., Wang Y., Lee H.K., Li Z. Non-fullerene acceptor photostability and its impact on organic solar cell lifetime. *Cell Reports Physical Science*. 2021. **2**(7): 100498.
28. Zanoni K.P., Pérez-del-Rey D., Dreessen C., Rodkey N., Sessolo M., Soltanpoor W., Bolink H.J. Tin (IV) Oxide Electron Transport Layer via Industrial-Scale Pulsed Laser Deposition for Planar Perovskite Solar Cells. *ACS Appl. Mater. Interfaces*. 2023. **15**(27): 32621.
29. AbdulWahhab N.A. Optical properties of $SnO_2$ thin films prepared by pulsed laser deposition technique. *J. Opt*. 2020. **49**(1): 41.
30. Saeed Z.A., Aadim K.A. Study of Optical, Structural and Morphology Properties of Tin Oxide Nanoparticles by Pulse Laser Ablation and its Effect on Bacteria Staphylococcus aureus. *Iraqi Journal of Science*. 2023. **46**(11): 5654.
31. Wan N., Lu X., Wang Y., Zhang W., Bai Y., Hu Y.S., Dai S. Improved Li storage performance in $SnO_2$ nanocrystals by a synergetic doping. *Sci. Rep*. 2016. **6**(1): 18978.
32. Garcia Romero D., Di Mario L., Yan F., Ibarra-Barreno C.M., Mutalik S., Protesescu L., Loi M.A. Understanding the Surface Chemistry of $SnO_2$ Nanoparticles for High Performance and Stable Organic Solar Cells. *Adv. Funct. Mater*. 2024. **34**(6): 2307958.


*Received 26.05.2024, accepted 25.11.2024*